FUPRE Journal of Scientific and Industrial Research
Vol.5, (2), 2021
ISSN: 2579-1184 (Print) ISSN: 2578-1129 (Online)

Cyber-Physical Quadcopter Surveillance System (CPQSS) Using 6-DoF in Tilting Rotors

Ugwoke F. N[1]. K. C. Okafor[2] , G. C. Ononiwu[3]
[1]Computer Science, Michael Okpara University of Agriculture, Umudike Abia State Nigeria
[2&3] Mechatronics Engineering, Federal University of Technology-Owerri, Nigeria
[1]ugwoke.fidelia@mouau.edu.ng, [2]kennedy.okafor@futo.edu.ng , [3]gordon.ononiwu@futo.edu.ng

Abstract
Generally, the need for holistic surveillance to preserve peace, orderliness, as well as safety of human lives is rapidly growing. Unmanned Aerial Vehicles (UAV) or quadcopters contend against external forces (like wind, gravity, and pressure) which determine design parameters. A candidate aerial quadcopter (surveillance) intervention fills this gap. In this case, Cyber-physical Quadcopter surveillance system (CPQSS) deployment is presented as a light-weighted drone with 6-degree of freedom (6-DoF) in tilting rotors. The active features and the baseline elements such as Quad-AI engine, propellers, electronic speed controllers, battery, flight time, power distribution, and flight controller are discussed. The integration and process logic for CPQSS is presented. Functional attributes of the quadcopter system with its implementation model have been verified especially the stability, flight-time, efficiency, and maneuverability. The system can serve as a convenient, efficient, and cost-effective alternative especially for crime-prone areas that require real-time monitoring.

Keywords—Cyber-Physical Systems, Cloud Robotics, Modeling, and Simulation,

I. INTRODUCTION

Unmanned aircraft, sometimes referred to as drones or multicopters are commonly employed in quick flights navigating easily through three-dimensional-projection with rotary arms (Lee, Lee & Chu, 2020). To date, a lot of work has been done on unmanned-aircrafts (UA) in various application fields including disaster monitoring, image-gathering, transportation logistics, military raids, among others (Lee, Lee & Chu, 2020; Hassanalian, Rice & Abdelkefi, 2018; Jeaong, Jo, Suk, Kim, Lee & Chung, 2018;Chao,Cao & Chen, 2020; Lee & Jin, 2016; Jawad, Jawad, Nordin, Gharghan, Abdullah & Abu-Alshaeer, 2019; Lu, Bagheri, James & Phung, 2018; Park, Lee, Eom & Lee, 2019;Wu,Yang, Xiao, & Guthbert, 2019). The absence of detailed parameterization is often a challenge in literature. Additionally, multicopters are constrained as it has limited battery capacity. Interestingly, the technology needed for optimizing batteries during flight is still evolving (Nguyen, Saussie & Saydy, 2020)(Yashin, Egorov, Darush, Zherdev &Tsetserukou, 2020).

A country like Nigeria needs lots of multicopter or drones to fix security issues ranging from kindnapping, herdsmen-terrorism, armed robbery, among others. Hence, an understanding of both design parameters and optimal techniques for UA systems is very important in this study.

Nigeria is Africa's most populous country with a population of over two hundred million people as of March 5th, 2021 (Statista, 2021). This large

number creates a huge demand for law and order enforcement agents. The various crisis including militancy, Fulani herdsmen, Boko haram sect, kidnapping, and all other forms of crimes. In the past decade, uncontrolled terrorism, crime, and violence have been the order of the day in our nation. This has led to gross damage to infrastructures and the shutdown of already existing facilities. Nigeria is a place where oil generates about 70% of government revenue while the other sectors have been left idle, now have the opportunity of focusing on agriculture and other sectors with the aid of drones.

For any purpose, surveillance quadcopters are mostly faced with major issues of stability, flight time, range, and maneuverability. The issue of stability, which could be a result of improper motor and propeller balancing or error/poor control with proportional integral derivatives (PID) calculations, and settings in the flight control program. The issue of range, which could lead to loss of transmission and crashing of the drone as a result of the poor transmitter to receiver connection/power. The issue of flight time, which could be due to the high ratio of the weight of the quadcopter to thrust of motors and propeller combination, low-efficiency motors, low capacity batteries, and other unnecessary power-consuming parts.

Closely related efforts on robotic quadcopters have been highlighted in the literature. For instance, collision avoidance scenarios in multicopters have been used to solve geometrical constraints and kinematics equation problems (Thanh & Hong, 2018). The authors in Dai, Quan, Ren & Cai, (2019)Dai, Quan, Ren & Cai, (2019b) discussed optimal aspects of a propulsion system that maximizes multi-copter efficiency. The work of Chen (2019) reported a monocular vision-based procedure applied in identifying obstacles and obstacle-aware regions adapted for collision avoidance by a multicopter. In Ghalamchi, Jia & Mueller, (2020), the authors worked on propeller degradation on a multicopter aerial robot. A representative sample of literature has been studied in Fu & Zheng (2020), Rectangular Pyramid Partitioning Using Integrated Depth Sensor(RAPPIDS) Bucki, Lee & Mueller,(2020), Robotic Landing Gear Sarkigov, Yashin, Tsykunov & Tsetserukou,(2018), Unmanned Aerial Vehicles (UAV) multi copter Platforms Lort, Aguasca, Lopez-Martinez & Marin,(2018), Multicopter Bauer, Hackl, Smedley & Kennel, (2018), Electric Multicopters Shi, Dai, Zhang & Quan (2017), and other related schemes in (Mintchev, de Rivaz & Floreano, 2017)(Pienaar, Reader & Davidson, 2017). Little has been done concerning Cyber-physical surveillance involving 6-DoF in 3-dimensional space.

In this paper, 6-DoF deals with the exact number of axes that a tilting rotor freely moves in 3-dimensional space. This determines the isolated parameters for the system.These works seek to develop an optimal quadcopter with improved stability, and optimized flight time with accurate control positioning using several sensors. Also, the work will focus on how to improve the stability of the quadcopter in flight, extend flight time and increase the range of transmission which would aid our campus-wide surveillance system. It also aims at adding some extra features like a return to home function, smartphone control, and hand gesture control if time and resources permit. The aim of this work aims to design and construct a surveillance quadcopter that supports the rotor title using 6-DoF. This will involve the design and implementation of optimal CPQSS that provides the following:

- Improved (very high) level of stability.
- Flight time of 30 minutes when fully charged.
- Maneuverable design with 6-DoF.

Additionally, it will have a communication (transmitter and receiver) system to achieve:

- Improved remote control and communication range of 1 km radius through the use of 2.4 GHz high power RF modules.
- Return to home (point of take-off) function.
- Installed visual display unit on the transmitter to display a first-person live telemetry view pilot system from the onboard camera and flight/quadcopter details like signal strength, battery level, altitude, and distance from home (point of take-off). Fail-safe in case of loss of signal.

II. SYSTEM DESIGN

In designing the system, artificial intelligence (AI) engine processor (Arduino Nano and QRB5165) was employed with granular C++ scripts. Using modular routing and fitting approaches, this offers both vertical and horizontally scaled process architecture for deep learning workloads. This enabled optimal and scalable supports for massive computation of all Quadcopter instances. Essentially, the motor specification which determines the total weight of the quadcopter is considered. This is used in deriving the thrust required to lift the quadcopter. A general rule is that the motors should be able to provide twice as much thrust as the weight of the quad. The design was done to provide sufficient thrust by the motors. The idea is to avoid take-off difficulties.

A. Requirements Engineering

By using the upthrust model below, gives
Thrust per motor = (weight 2) / 4
(For 2:1 thrust/weight ratio)
Where: weight = estimated weight of loaded quadcopter which is obtained by adding the individual weights of all motors, propellers, ESCs, camera, IMU, etc.

To get the estimated weight of the quadcopter, the method of research is done by first researching UAV, multicopter, and especially quadcopter. By using gathered knowledge and information an approximation of the quadcopter weight is made based on some of the main components needed. This can be seen in Table I.

TABLE I. QUADCOPTER COMPONENTS WEIGHT ESTIMATION

S/N	Quad-Components	Unit weight estimation/unit	No of Units	Weighted sum
1	Brushless-motors	62	4	248
2	Propellers	18	4	72
3	LiPo batteries	362	2	724
4	ESCs	20	4	80
5	Frame & landing gear	400	1	400
6	Camera & MinimOSD	20	1	20
7	FPV transmitter	30	1	30
8	GPS receiver	30	1	30
9	IMU & Arduino nano	16	1	16
10	RF receiver, antenna & pro mini	20	1	20
11	Other accessories (jumpers, screws, tapes, etc)	50	1	50

For the quadcopter to hover, it has to subdue gravity. Since the estimated weight of the quadcopter is 1690 g, its motors have to produce a combined thrust greater than 1690 g to beat gravity and take off. In other words, each motor has to produce at least: 1690/4 = 422.5 g (assuming that all the motors/propellers produce an equal amount of thrust).

Since it is recommended and also a general rule to have a 2:1 thrust: weight ratio for a standard quadcopter, the standard thrust therefore required for each motor is obtained using 422.5 g x 2 = 845 g.

The selection of motors was then realized using this information guide. When selecting motors, there are usually specifications that come with the motor either provided by the manufacturer as highlighted:
Motor Specifications:
Model: SunnySky X2212 980 KV
Kv: 980 rpm/v
Max current: 17 A
Max Power: 205 W @ 12 V (3S)
Weight: 56 g
Cell count: 3S~4SLipoly

B. Propeller

In the proposed CPQSS, the quadcopter makes use of two-clockwise (CW) and two

counterclockwise (CCW) propellers. These are classified by length and pitch. For example, 9×4.7 propellers are 9 inches long and have a pitch of 4.7. Generally, increased propeller pitch and length will draw more current. Also, the pitch can be defined as the travel distance of one single prop rotation. In a nutshell, higher pitch means slower rotation but will increase vehicle speed which also uses more power. A higher pitch propeller moves a greater amount of air, which could create turbulence and cause the aircraft to wobble during hovering. Therefore, the need to find a good balance between length and pitch when selecting propellers. In consideration of thrust required and stability, a set of 10 x 4.5 propellers and 11 x 4.5 propellers was chosen. This would enable a range of tests on thrust, stability, payload capacity, and flight time. This set of propellers also include two blade sets and three-blade sets of carbon-fiber propellers.

C. Electronic Speed Controller

The ESC converts the battery pack DC voltage to a three-phase alternating signal which is synchronized to the rotation of the rotor and applied to the armature windings. The motor speed is set by the ESC in response to a pulse width modulated control signal. The motor speed is then proportional to the root-mean-square (RMS) value of the armature voltage. When considering the ESCs for quad motors, the motor amperage is seriously considered. For instance, the identified motor draws a max of 17 A. Hence, it is imperative to use a speed controller with an amperage greater than 17 A. The computation model is applied using (1):

$$(1.2 – 1.5) \times I_{max} \quad (1)$$

Where: I_{max} = 17A, Then, (1.2 – 1.5) x 17 A = (20.4 – 25.5) A

Therefore, an ESC within the range of 20 to 25 A can be used together with this motor comfortably. Considering cost and efficiency, a SimonK 20 A (continuous 20 A, burst 30 A up to 10 secs) electronic speed controller (ESC) with battery eliminated circuit (BEC) output of 5 V/3 A was chosen. This BEC output (5 V/3 A) can be used to power up the other onboard electronics like the microcontroller (flight controller board), the camera, the FPV transmitter, the radio receiver, etc. With this motor, propeller, and electronic speed controller combination, and based on the calculations carried out so far, the thrust required can be handled comfortably. This setup would enable the quadcopter to realize its full potential with room for more load if necessary.

D. Battery

To get the best flight time and performance, the Lipo battery is selected as it achieves longer flight times. The largest battery (in terms of capacity) that could support the maximum takeoff weight of the quadcopter was considered. The physical size of the battery was also considered for proper balance. A larger battery allows for a longer flight time. Unfortunately, the increase in flight time is not proportional to the increase in battery size. This implies that as the battery gets larger, the increase in flight time becomes ineffective. Eventually, it will reach a point where it just doesn't gain any more flight time with a bigger battery (even lose flight time). This is mainly caused by the weight of the battery.

The most important factor considered is the battery discharge C rating that was the optimum for the quadcopter. A discharge rate (C rating) that is too low, can result in the battery being damaged, and the quadcopter under-performing because the battery can't release current fast enough to power motors properly. Since higher C rating batteries are heavier, using a battery that has a C rating that is too high, the quadcopter will just be carrying extra weight around, ultimately reducing the flight time. The tradeoff between flight time and battery capacity makes it more difficult to choose which battery should be used, rather than just "pick the largest battery available". To know the optimum battery to use, the total current draw of the system is first calculated using the data from the motors.

The total current draw of the system is computed thus:
Quad-motor Maximum power = 191 W
Battery voltage (3S-LiPo) = 3 x 3.7 V = 11.1 V
Where 3.7V = Quad-nominal voltage for respective cells)
Max motor current draw = 191 W/11.1 V = 17.2 A per motor
For 4 motors => 17.2 x 4 = 68.8 A.

Therefore a 3S battery pack having amperage above 68.8 A is needed. Considering a 3 cell LiPo battery pack selected in respect of these specifications:
Battery capacity = 5 Ah
Discharge rate = 25 C
Voltage (3S) = 3 cells x 3.7V = 11.1 V
Max continuous Amp draw (A) = Battery capacity (Ah) x discharge rate (C) = 5 Ah x 25 C = 125 A

Running two of these batteries in parallel would further increase the capacity of the 3S LiPo pack giving a whopping 10 Ah (2 x 5 Ah). Max continuous Amp draw (A) = 10 Ah x 25 C = 250 A. This implies that the batter amperage is more than that of the four motors, thereby accounting for efficient design.

E. Flight Time

There is a strong relationship between the vehicle weight and the battery run time. With this, the estimated flight time of the quadcopter can be determined. Since the design is aimed at maximizing flight time, data would be used in slow flight and hover use cases without any aggressive motions. Granting that the estimated thrust per motor is 845 g (at full throttle), therefore at 50% throttle, this gives 422.5 g (which is the least amount of thrust per motor). The thrust of 422.5 g per motor is used because at this point, the quadcopter lifts and hovers. The total computed time from the manufacturers' datasheet was 26.27 minutes. This implied that the quadcopter should be able to hover and fly around slowly for about 26 minutes. The actual flight time may vary as this is only an estimate.

F. Power Distribution

For the direct supply, the battery (which is a 3S 9000 mAh LiPo pack) is interfaced with the power escalation dashboard. The power distribution is divided into two, namely - Direct supply and Indirect supply. These provide 11.1 V directly to all four ESCs. These four ESCs regulate the power of the motors based on control data. For the indirect supply, the ESCs which feature an inbuilt battery eliminator circuit (BEC) steps down the 11.1 V supplied to 5 V/3 A. It then supplies this 5 V to the microcontroller, camera, video transmitter, radio control receiver (Arduino pro mini and NRF24L01 combo), and other accessories like lights. This 5 V is further reduced to 3.3 V for onboard sensors all of which can be seen in Fig. 1.

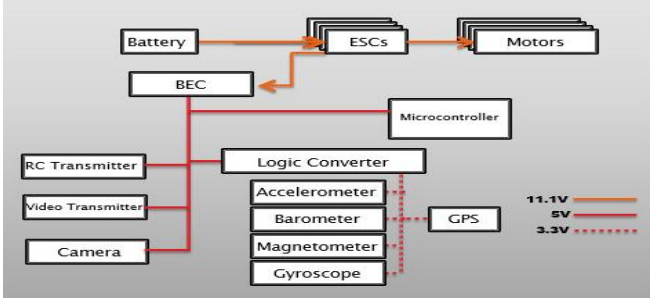

Figure 1. Distribution of power on the quadcopter

G. Flight Controller

The primary flight controller is the Arduino Nano V3.1. It is a small, complete, and breadboard-friendly computer based on the 8-bit ATmega328p chip at a frequency of 16 MHz with a 32 kB flash RAM. Fig. 2 shows the flight controller component mapping especially the input/output dependencies. The flight control circuit board consists of the microcontroller (Arduino nano V3.1) and the GY-80 IMU (including accelerometer, gyroscope, compass, and barometer).

Table II shows a list of the tuning parameters used for the dynamic simulations of the quadcopter. The PID gains used in the altitude controller are detailed as well in Table III. Similarly, the PID gains of the position controller are shown in Table IV.

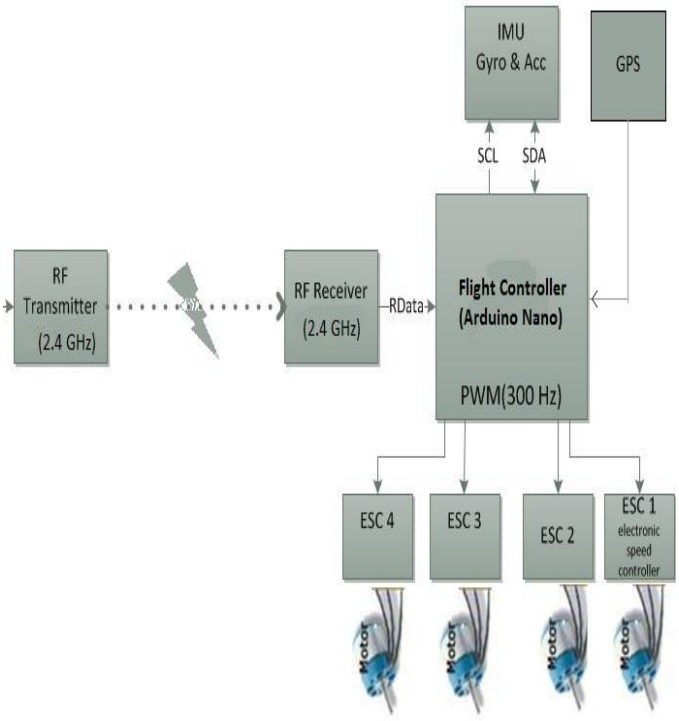

Figure 2. Quadcopter Flight Controller Architecture.

TABLE II. SUMMARY OF SELECTED COMPONENTS FOR CQPSS

Component	Description
Frame	The Centre plate is high-quality glass fiber while the arms are constructed from ultra-durable polyamide nylon. Width: 450mm Height: 55 mm
Brushless Motor	SunnySky X2212 980 KV brushless out-runner motor.
ESC	SimonK 20 A (continuous 20 A, burst 30 A up to 10 secs) electronic speed controller (ESC) with battery eliminated circuit (BEC) output of 5 V/3 A.
Battery	Two Flouren 4.5 Ah 30 C 3S LiPo batteries in parallel giving us a 9 Ah 30 C 3S LiPo pack.
Propellers	10 x 4.5 and 11 x 4.5-inch carbon fibre propellers.
Flight Controller	Arduino Nano V3.1 and GY-80 IMU.
GPS	NEO-6M V3.1 and I^2C to GPS NAV Module.

TABLE III. ALTITUDE CONTROLLER PID PARAMETRIC GAINS

Parameter	Proportional gain, *kp*	Integral gain, *ki*	Differential gain, *kd*
Pitch, Θ	3.3	0.030	23
Yaw, ψ	6.8	0.045	0
Roll, ϕ	3.3	0.030	23
Altitude, Z	6.4	0.025	24

TABLE IV. POSITION CONTROLLER PD PARAMETRIC GAINS

Parameter	Proportional gain, *kp*	Integral gain, *ki*	Differential gain, *kd*
Position	0.15	0	0
Position Rate	3.4	0.14	0.053
Navigation Rate	2.5	0.33	0.083
Level	9.0	0.010	100
Mag	4.0	0	0

The CPQSS was achieved with 6-DoF per arm (roto-tilt) for the entire system. The quadcopter is modeled to move in 6-DoF relative to the physical world. For the rotors to move, a revolute joint and a controlled torque were added to the system, while the gravity acting on the system is added to allow for proper simulation. This function was implemented in Fig. 3 while Fig. 4 shows the loop PID diagram.

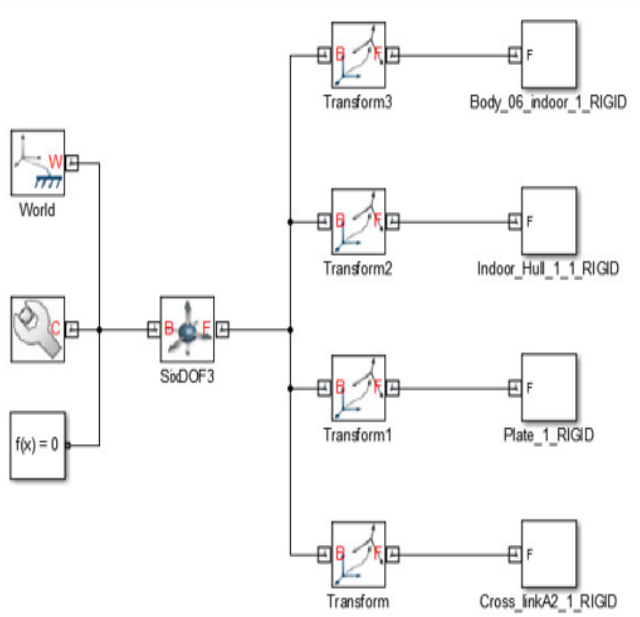

Figure 3a.Quadcopter process logic model: The 6-DoF system model

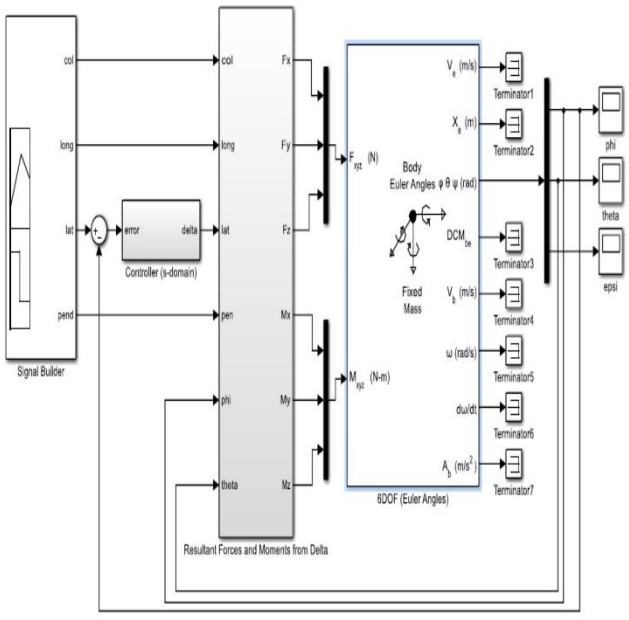

Figure 3b. Quadcopter process logic model: Non-Linear Control Block

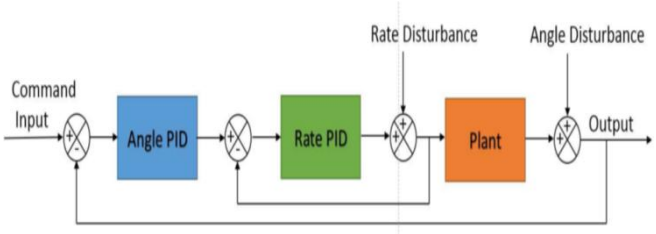

Figure 4. Quadcopter inner and outer loop PID diagram

Table IV: Initial PID values to stabilize roll and pitch

	Roll/Pitch Angle Gains	Roll/Pitch Rate Gains	Yaw Rate Gains
K_p	3.604	0.2209	0.1141
K_i	0	0	0.6340
T_d	0	0.014	0

The closed-loop response of the quadcopter system with the PID values from Table 4.1 IV is shown in Fig. 5. It is clear from Fig. 5 that roll, pitch, and yaw responses are stable and return to the trim value at zero within a second. Since there is no closed-loop control on position, translational motion(x, y, z) of the quadcopter will have small steady-state errors, which are relatively small and therefore negligible.

III. CQPSS CAD

In this paper, the CQPSS with 6-DoF design encapsulates the frame, brushless DC motors, power supply, rotors, and flight control circuit board as shown in Fig. 3. The Computer-aided design of the frame was done using Solidworks 2014 SP1.0 modeling tool for precise and accurate measurements. Its features include 3D modeling. The dimensions considered are 450 mm width, 55 mm height (without landing skid), 295 g weight (without electronics and landing skid), and 16/19 mm motor mount bolt holes. After each component was modeled, these were coupled together to form an assembly in the assembly creation window. The weights of the different parts from the design specification were ascertained from the type of material used (plastic, fiberglass, etc.), the density of the material, length, width (or diameter), and height of the component. This was done by the software.

The design Implementation was done in five stages:

- Construction of the quadcopter chassis.
- Initial Setup and Programming of the microcontroller and ESCs.
- Programming of the radio transceivers and configuration of FPV transmitter and receiver.
- Motor and propeller balancing.
- Final build, mounting of components, and testing

It is clear from Fig. 5 that roll, pitch, and yaw responses are stable and return to the trim value at zero within a second. Since there is no closed-loop control on position, translational motion(x, y, z) of the quadcopter will have small steady-state errors, which are relatively small and therefore negligible.

Fig.6*a-i*, shows the quadcopter after all the components had been securely and properly placed and ready for testing.The closed-loop response of the quadcopter system with the PID values from Table IV is shown. Fig. 6*j* shows the realized design as proof of concept. Future works will explore advanced concepts in (Okafor & Obayi, 2020; Okafor, Achumba, Chukwudebe & Ononiwu, 2017; Okafor, Guinevere & Akinyele, 2011; Okafor, 2011) to enhance the CQPSS.

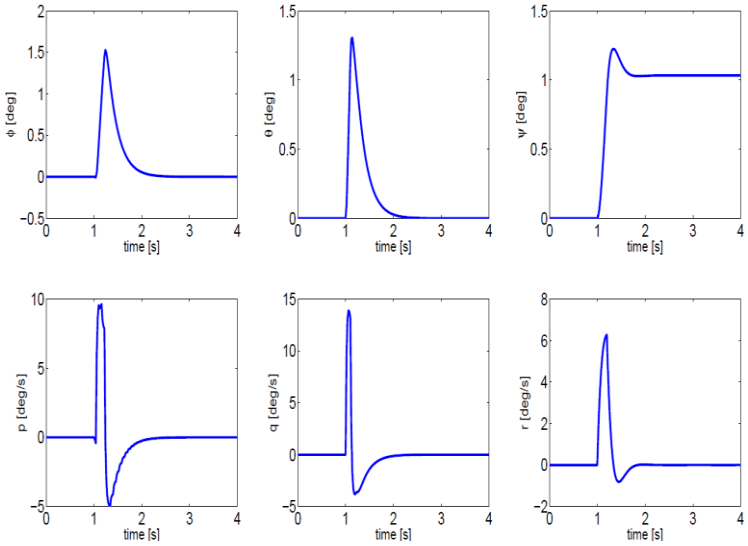

Fig 5. Impulse response of closed-loop PID quadcopter dynamics.

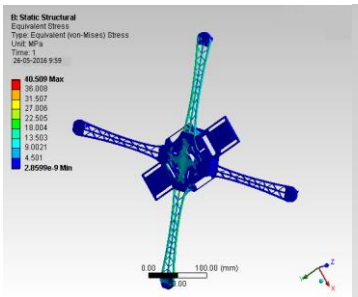


a) CPQSS Frame design b) Propeller Model


c) Arm Model d) landing gear model


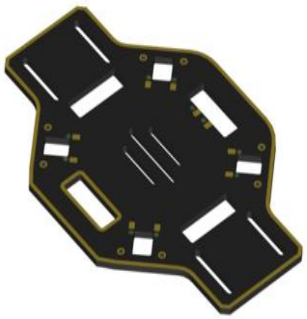

e) Motor Model f) Bottom Plate Model

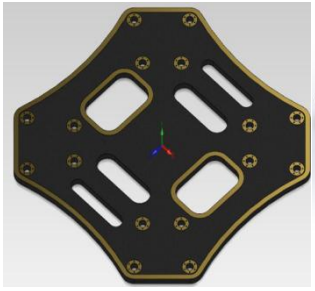
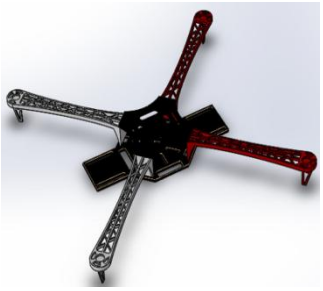

g) Top Plate mOdel h) Assembly frame


i) Completed CPQSS j) Deployed model

Figure 6a-j. Optimal Quadcopter design after final component population

IV. SUMMARY DISCUSSIONS

After the implementation and testing of the quadcopter in Fig. 5, the following objectives were achieved in Fig 6j.

i. The quadcopter was able to meet its weight requirement with its approximate weight being 1.57 kg.
ii. The quadcopter was able to achieve an improved (very high) level of stability.
iii. Flight time of 22 minutes 15 seconds.
iv. Maneuverable design with 6-DoF.
v. Remote control with a communication range of +1km radius through the use of 2.4 GHz high power RF modules.
vi. Installed visual display unit on the transmitter to display a first-person live telemetry view pilot system from the onboard camera and flight/quadcopter details like signal strength, battery level, altitude, and distance from home (point of take-off).
vii. Fail-safe in case of loss of signal.
viii. Return to home (point of take-off) function.
ix. Autonomous GPS waypoint missions.

V. CONCLUSION

This paper has modeled a non-linear efficient frame-control of a CPQSS through pitch, roll, yaw, and thrust window configurations. The computation and derivation details especially for the nonlinear model of CPQSS dynamics were presented. A 6-DoF motion is introduced (through tilting rotors) with a non-linear model for the initial linearization towards an equilibrium threshold. The 6-DOF kinematics is implemented in the design to stabilize and track the control of

three angular motions (Pitch, Yaw, and roll). The process transfer function of the respective DoF rotation dynamics shows that the design is efficient without any damping factor in linear mode. The work equally employed a PID controller for collaborative assistance to control and stabilize the 6-DoF rotations.

The controls of the actuators were demonstrated through simulation use-cases. The simulated and experimental results are satisfactory for the Proof-of-Concept.

REFERENCES

Lee C., Lee S. & Chu B. (2020). Extension of Quadcopter Flight Range Based on Quadcopter Transport System and Autonomous Ramp Flight Algorithm. *IEEE Access, 8, 156422*-156432, doi: 10.1109/ACCESS.2020.3019066. M.

Hassanalian D., Rice & Abdelkefi A. (2018). Evolution of space drones for planetary exploration: A review. *Prog. Aerosp, 97*, 61-105.

Kim S.-H., Lee D.-K., Cheon J.-H., Kim S.-J. & Yu K.-H. (2016). Design and flight tests of a drone for delivery service. *J. Inst. Control Robot. Syst*., *22*(3), 204-209.

Jeaong H., Jo S., Suk J., Kim S., Lee Y.-G. & Chung I. (2018). Modeling of aerodynamic database and robust control using disturbance observer for quadcopter. *J. Inst. Control Robot. Syst*., *24*(6), 519 531.

Chao H., Cao Y. & Chen Y. (2010). Autopilots for small unmanned aerial vehicles: A survey. *Int. J. Control Autom. Syst*., *8*(1), 36-44.

Lee J. & Jin T. (2016). Tracking of walking human based on position uncertainty of dynamic vision sensor of quadcopter UAV. *J. Inst. Control Robot. Syst.*, *22*(1), 24-30.

Jawad A.M., Jawad H.M., Nordin R., Gharghan S.K., Abdullah N.F. & Abu Alshaeer M.J.(2019).Wireless power transfer with magnetic resonator coupling and Sleep/Active strategy for a drone charging station in smart agriculture. *IEEE Access, 7*, 139839-139851.

Lu M., Bagheri M., James A. P. & Phung T. (2018).Wireless charging techniques for UAVs: A review reconceptualization and extension. *IEEE Access*, 6, 29865-29884.

Park J., Lee H., Eom S. & Lee I. (2019).UAV-aided wireless powered communication networks: Trajectory optimization and resource allocation for minimum throughput maximization. *IEEE Access, 7* 134978-134991.

Wu F., Yang D., Xiao L. & Cuthbert L. (2019). Energy consumption and completion time tradeoff in rotary-wing UAV enabled WPCN. *IEEE Access, 7*, 79617-79635.

Nguyen T., Saussie D. & Saydy L. (2020). Design and Experimental Validation of Robust Self-Scheduled Fault-Tolerant Control Laws for a Multicopter UAV. *IEEE/ASME Transactions on Mechatronics*, doi: 10.1109/TMECH.2020.3042333.

Yashin G., Egorov A., Darush Z., Zherdev N. & Tsetserukou D. (2020). LocoGear: Locomotion Analysis of Robotic Landing Gear for Multicopters. *IEEE Journal on Miniaturization for Air and Space Systems, 1*(2)138-147, doi: 10.1109/JMASS.2020.3015525.

Population in Africa, by country (2021). African countries with the largest population as of 2021(in 1,000 individuals). *Statista*, URL www.statista.com/statistics/1121246.

Thanh N.N & Hong S. K. (2018). Completion of Collision Avoidance Control Algorithm for Multicopters Based on Geometrical Constraints. *IEEE Access, 6*, 27111-27126, doi: 10.1109/ACCESS.2018.2833158.

Dai X., Quan Q., Ren J. & Cai K. (2019). Efficiency Optimization and Component Selection for Propulsion Systems of Electric Multicopters. *IEEE Transactions on Industrial Electronics,66*(10), 7800-7809, doi: 10.1109/TIE.2018.2885715.

Dai X., Quan Q., Ren J. & Cai K. (2019b). An Analytical Design Optimization Method for Electric Propulsion Systems of Multicopter UAVs with Desired Hovering Endurance. *IEEE/ASME Transactions on Mechatronics, 24*(1), 228-239, doi: 10.1109/TMECH.2019.2890901.

Chen H. (2019). Monocular Vision-Based Obstacle Detection and Avoidance for a

Multicopter. *InIEEE Access, 7,* 167869-167883, doi: 10.1109/ACCESS.2019.2953954.

Ghalamchi B., Jia Z. & Mueller M.W. (2020). Real-Time Vibration-Based Propeller Fault Diagnosis for Multicopters. *IEEE/ASME Transactions on Mechatronics, 25*(1), 395-405, doi: 10.1109/TMECH.2019.2947250.

Fu Q. & Zheng Z.-L. (2020). A Robust Pose Estimation Method for Multicopters Using Off-Board Multiple Cameras. *IEEE Access, 8,* 41814-41821, doi: 10.1109/ACCESS.2020.2976733.

Bucki N., Lee J. & Mueller M.W. (2020). Rectangular Pyramid Partitioning Using Integrated Depth Sensors (RAPPIDS): A Fast Planner for Multicopter Navigation. *IEEE Robotics and Automation Letters, 5*(3), 4626-4633, doi: 10.1109/LRA.2020.3003277.

Sarkisov Y.S., Yashin G.A., Tsykunov E.V. and Tsetserukou D. (2018). DroneGear: A Novel Robotic Landing Gear with Embedded Optical Torque Sensors for Safe Multicopter Landing on an Uneven Surface. *IEEE Robotics and Automation Letters, 3*(3)1912-1917, doi: 10.1109/LRA.2018.2806080.

Lort M., Aguasca A., López-Martínez C. & Marín T.M. (2018). Initial Evaluation of SAR Capabilities in UAV Multicopter Platforms. *IEEE Journal of Selected Topics in Applied Earth Observations and Remote Sensing, 11*(1), 127-140, doi: 10.1109/JSTARS.2017.2752418.

Bauer F., Hackl C.M., Smedley K.M. & Kennel R.M. (2018). Multicopter with Series Connected Propeller Drives. *IEEE Transactions on Control Systems Technology, 26*(2),563-574, doi: 10.1109/TCST.2017.2679071.

Shi D., Dai X., Zhang X. & Quan Q. (2017). A Practical Performance Evaluation Method for Electric Multicopters. *IEEE/ASME Transactions on Mechatronics, 22*(3), 1337-1348, doi:10.1109/TMECH.2017.2675913.

Mintchev S., de Rivaz S. & Floreano D. (2017).Insect-Inspired Mechanical Resilience for Multicopters. *IEEE Robotics and Automation Letters, 2*(3), doi: 10.1109/LRA.2017.2658946.

Pienaar H., Reader H.C. & Davidson D.B. (2017). Karoo Array Telescope Berm Shielding: Efficient Computational Modeling and Multicopter Measurement. *IEEE Transactions on Electromagnetic Compatibility,59*(2), 375-382, doi: 10.1109/TEMC.2016.2618911.

Okafor K.C & Obayi A.A. (2020). Industry 4.0 CAMI: An Elastic Cloud Zynq UltraScale FPGA Metering Architecture", *Lecture Notes in Computer Science (including subseries Lecture Notes in Artificial Intelligence and Lecture Notes in Bioinformatics*), 2020, 12254 LNCS, *12254*, 527–543, Print ISSN: 03029743, 16113349.

Okafor K.C., Achumba 1.E., Chukwudebe G.A & Ononiwu G.C. (2017). Leveraging Fog Computing For Scalable IoT Datacenter Using Spine-Leaf Network Topology. *Journal of Electrical and Computer Engineering, 2017*, 1-11, DOI:10.1155/2017/2363240.

Okafor K.C., Guinevere, E.C. & Akinyele, O.O. (2011). Hardware Description Language (HDL): An Efficient Approach to Device Independent Designs for VLSI Market Segments. *In Proc. 3rd IEEE International Conference Adaptive Science and Technology (ICAST),* 262 – 267, Abuja, 24th-26th.

Okafor K.C. (2021). Dynamic Reliability Modelling of Cyber-Physical Edge Computing Network. *International Journal of Computers and Applications, (IJCA), SI- Sustainable Computing for Intelligent Systems, United Kingdom, 43*(7), 612 - 622 Print ISSN: 1206 212X Online ISSN: 1925-7074.

Okafor K.C., Guinevere, E.C. & Akinyele, O.O. (2011). Hardware Description Language (HDL): An Efficient Approach to Device Independent Designs for VLSI Market Segments. *In Proc. 3rd IEEE International Conference Adaptive Science and Technology (ICAST),* 262 – 267, Abuja, 24th-26th